EMBO J

Supplemental Information

RPA facilitates telomerase activity at chromosome ends in budding and fission yeasts.

Pierre Luciano, Stéphane Coulon, Virginie Faure, Yves Corda, Julia Bos, Steve Brill, Eric Gilson, Marie-Noelle Simon, and Vincent Géli.

LEGENDS TO SUPPLEMENTARY FIGURES

Figure S1 (complementary to Fig. 1). Binding of RPA to telomeric DNA in WT and *mre11*Δ cells.

RPA telomeric binding of samples from Fig1D and E was analysed by qRT-PCR using telomeric primers (Tel XV-L) and non telomeric primers (Gal2A). Graphs represent the fold enrichment ((IP/Input$_{\text{Tel XV-L}}$) / (IP/Input$_{\text{Gal2A}}$)) of RPA telomeric binding in WT (A) and *mre11*Δ cells.

A)

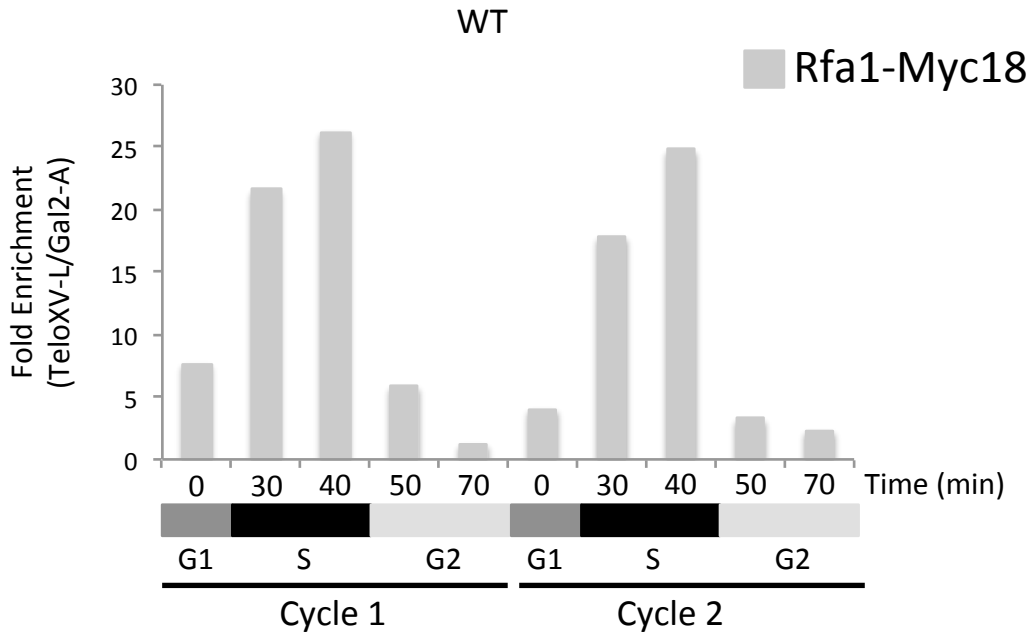

B)

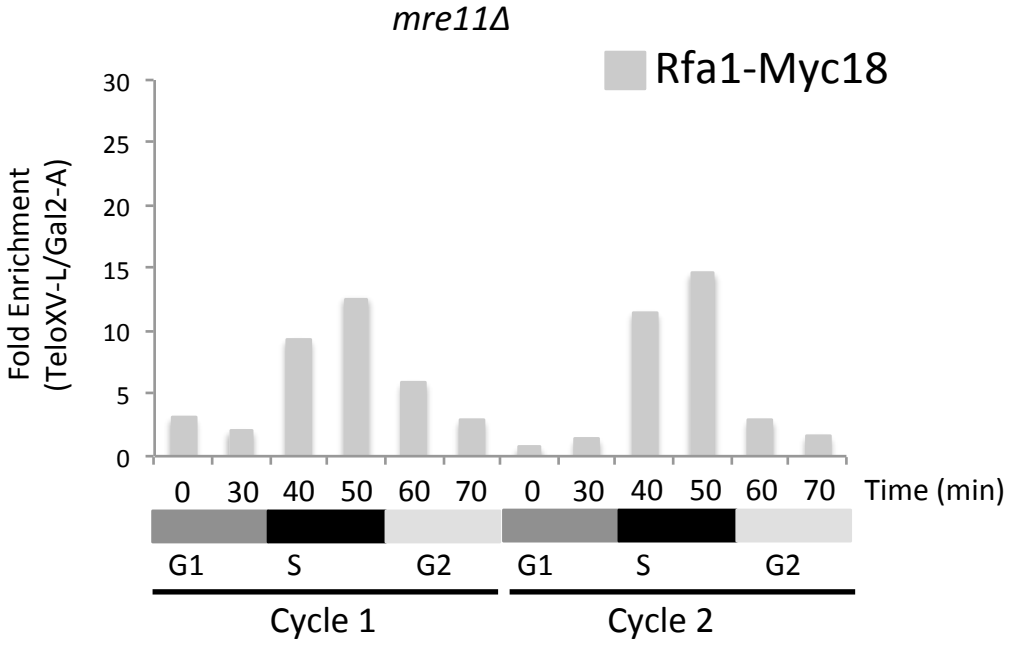

Figure S2. (A) U1 SnRNA does not co-precipitate with RPA. Immunoprecipitations (IP) were carried out using anti-Myc antibodies on cell extracts prepared from cells expressing the indicated proteins. RNAs associated to the IP were extracted and analyzed by reverse transcriptase assays followed by PCR with primers specific for *U1 SnRNA*. (B) Protein extracts from a wild-type strain were treated with either RNase or DNase and IPs were performed with anti-Rfa2 antibodies. The presence of TLC1 in the immunoprecipitates was analyzed as in Fig. 2.

A

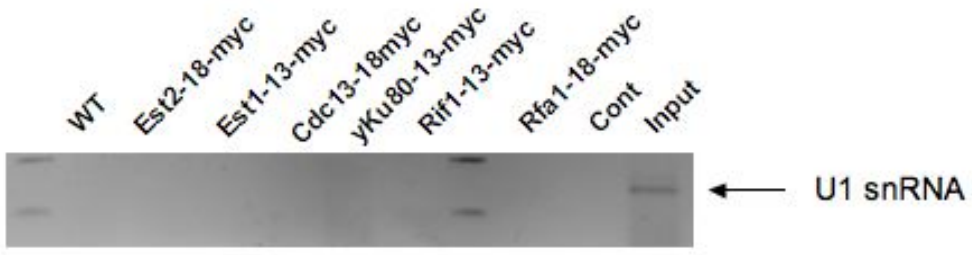

B

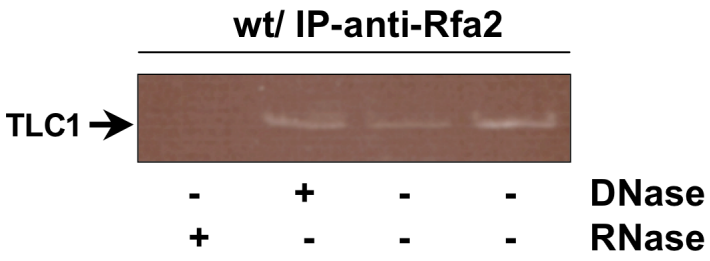

Figure S3. Modelling the *rfa1-D228Y* mutation.

(A) Domain organisation in the heterotrimer RPA70/RPA32/RPA14. Association of RPA with ssDNA is mainly mediated by the RPA70 OB fold A, B, C and RPA32 OB fold D.

(B) Modelling the position of the Rfa1-D228Y mutation from the structure of the human RPA-A/RPA-B OB fold. The position of ssDNA in the conserved groove of the domain is shown (from Bochkareva et al., 2002). The aspartic acid at position 228 (mutated in tyrosine in the Rfa1-D228Y) is invariant in RPA70 alignments. According to the published structure of Rfa1 (Bochkareva et al., 2001), this residue is thought to play a structural role at the periphery of the second OB fold of Rfa1, particularly at the first helix turn of OB-B. The D228 residue appears to be not directly accessible at the surface of the protein, however its mutation into tyrosine should destabilize locally a conserved surface region. This conserved region, that is different from the canonical OB fold region involved in the binding of the ssDNA, could be implied in an interaction with another partner than ssDNA.

(A)

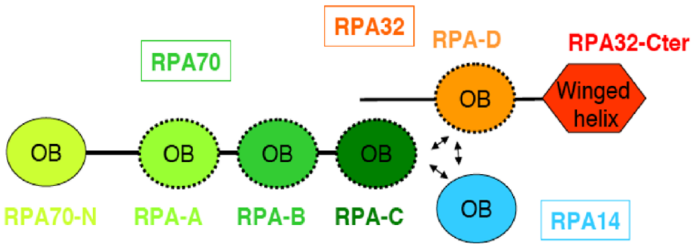
RPA32
RPA-D
RPA32-Cter
RPA70
OB
Winged helix
OB
OB
OB
OB
OB
RPA70-N
RPA-A
RPA-B
RPA-C
RPA14

(B)

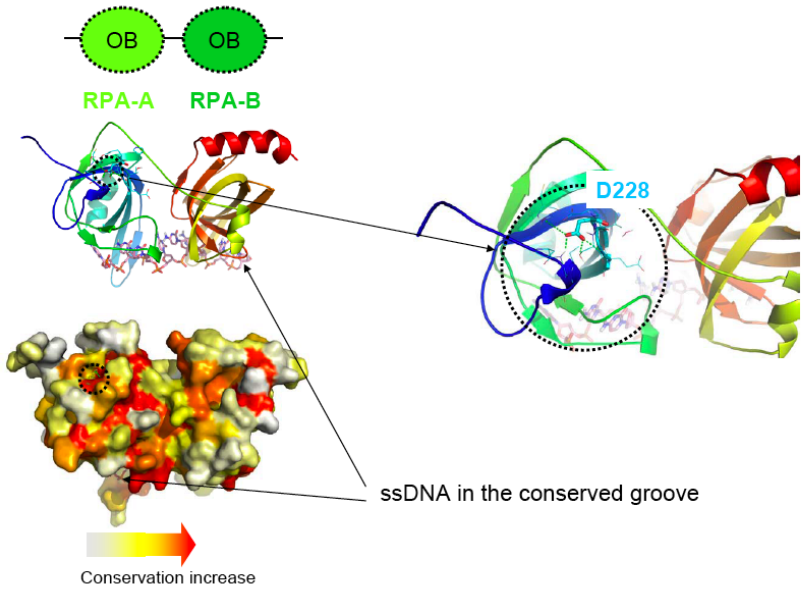
OB
OB
RPA-A
RPA-B
D228
ssDNA in the conserved groove
Conservation increase

Figure S4. Telomere length of the *tel1*Δ *rfa1-D228Y double mutant*. Diploids *RFA1/rfa1D228Y TEL1/tel1::LEU2* were sporulated and telomere length of 2 tetratype tetrads was analyzed, after five restreaks, by Southern blot using a T-G_{1-3} probe.

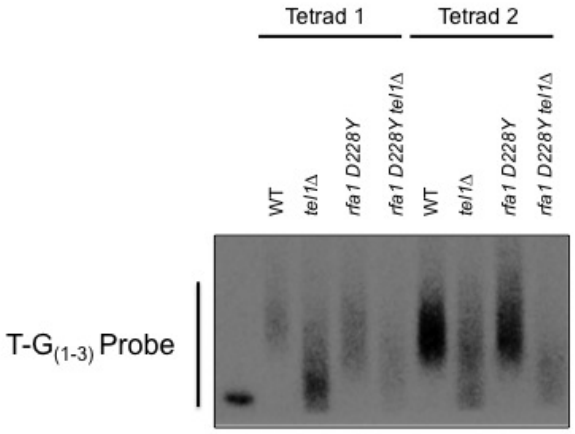

Figure S5. RPA and Cdc13 telomeric binding in WT and *rif1*Δ *rif2*Δ cells. (A) WT and *rif1*Δ *rif2*Δ cells expressing *Cdc13-Myc13* were harvested at the indicated times after release from an alpha-factor block. Cell cycle progression was followed by FACS (NS: non synchronized). (B) Telomeric DNA binding of Cdc13-Myc13 and Rfa1 was monitored by ChIP performed with anti-Myc and anti-Rfa1 antibodies, respectively, from cells harvested at the indicated times. The input DNAs (2 μl) and DNAs associated to the Cdc13-Myc13 and Rfa1-ChIPs (20 μl) at each time point were spotted onto a Hybond-N^+ membrane, crosslinked by UV treatment and hybridized with a radioactive telomeric (TG_{1-3}) probe. (C) The amounts of telomeric DNA in the Cdc13-Myc13 and Rfa1-ChIP DNA normalized to the input telomeric DNAs are represented. (D) At each time point, immunoprecipitations with anti-Rfa1 antibodies were carried out from protein extracts prepared from the same cultures than those used for the ChIP. RNAs associated to the IPs were extracted and analyzed by RT-PCR with primers specific for TLC1.

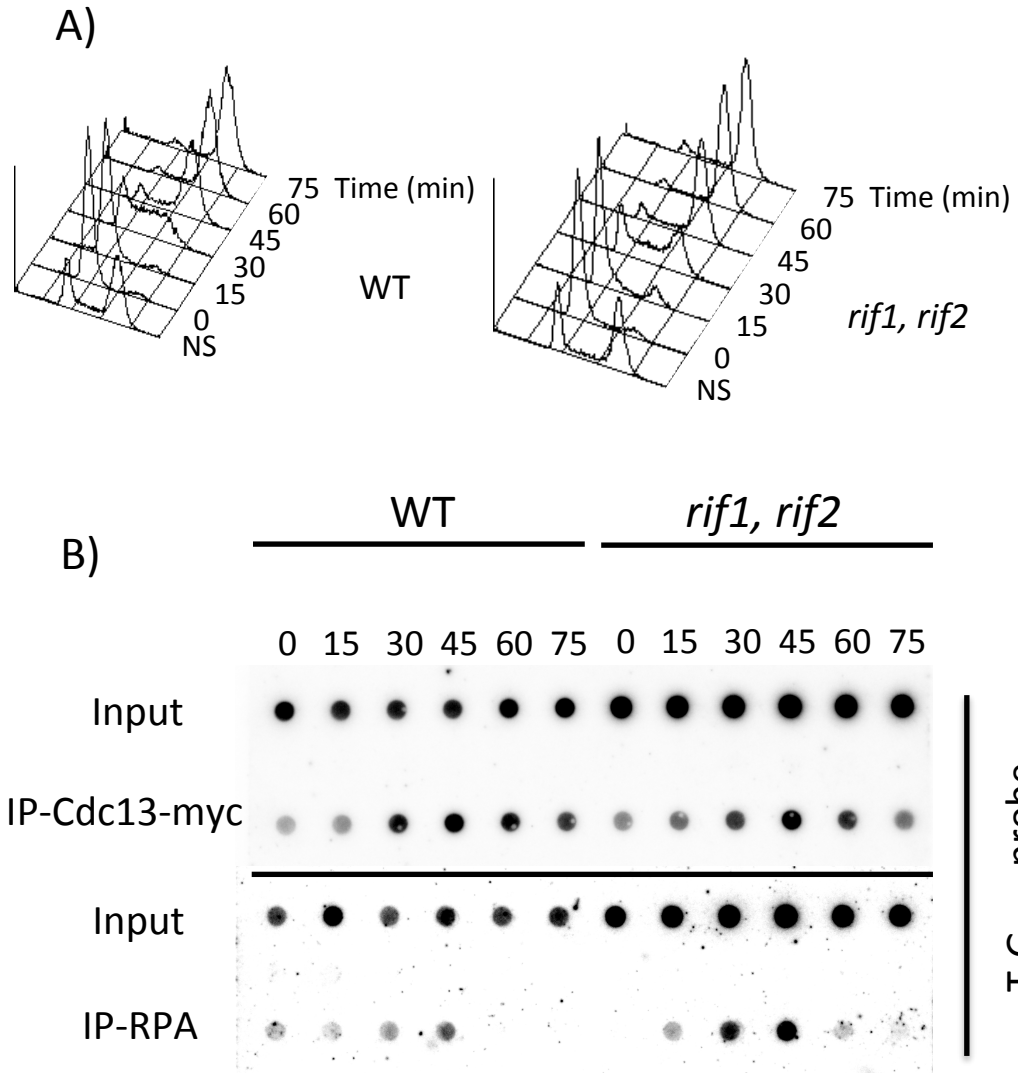
A)
75 Time (min)
60
45
30
15
0
NS
WT
75 Time (min)
60
45
30
15
0
NS
rif1, rif2
B)
WT
rif1, rif2
0 15 30 45 60 75 0 15 30 45 60 75
Input
IP-Cdc13-myc
Input
IP-RPA
T-G(1-3) probe

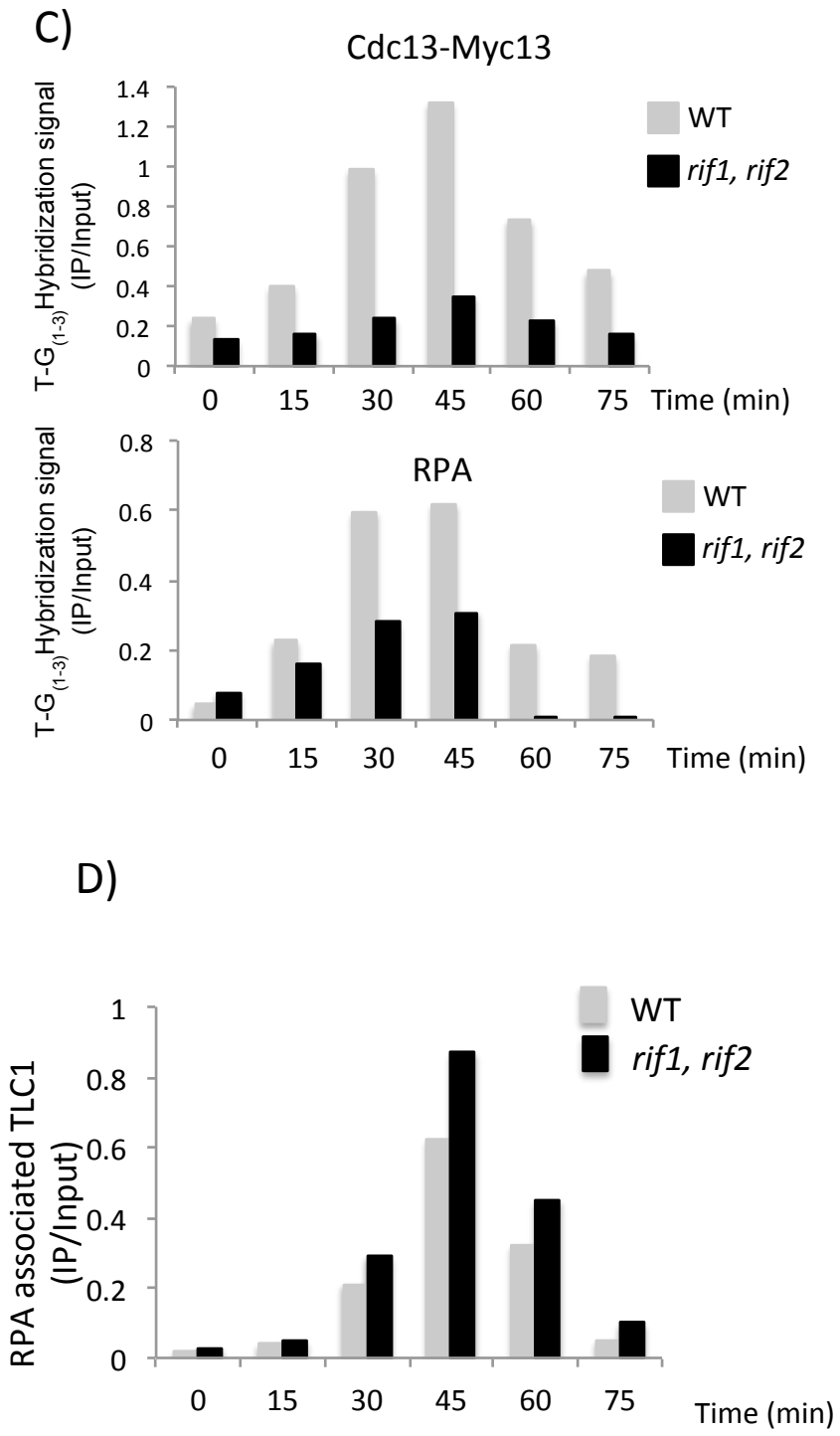

Figure S6.

Telomere length of the *rfa2Δ40* mutant. In this supplemental figure, we have revisited the phenotype associated to the *rfa2Δ40* mutant described in our previous study (Schramke et al., 2004).

(A) Construction of the *rfa2Δ40* mutant. The deletion removing the *RFA2* intron and the region extending from codon 3 to codon 39 of *RFA2* (nt 7 to

228) was performed as described in the scheme below. By replacing endogenous *RFA2* with the *rfa2Δ40* mutant allele, we generated an allele encoding a truncated protein extending from residue 1 to 165 (*rfa2**) that is co-expressed with *rfa2Δ40*. To eliminate potential effects of *rfa2**, this non-functional truncated allele was fully disrupted with a *KAN-MX4* marker. The resulting strain produces *rfa2Δ40* as the sole form of Rfa2. As a control, we did exactly the same construction but instead of removing the RFA2 intron and the region extending from codon 3 to codon 39, we removed only the intron (region from nt 7 to 115).

(B) Telomere length of the *rfa2Δ40* mutant. Telomere length of W303 and YPH250 strains bearing the indicated alleles. Note the appearance of revertants in the YPH250 *rfa2Δ40* mutant showing WT telomeres and also normal growth.

A

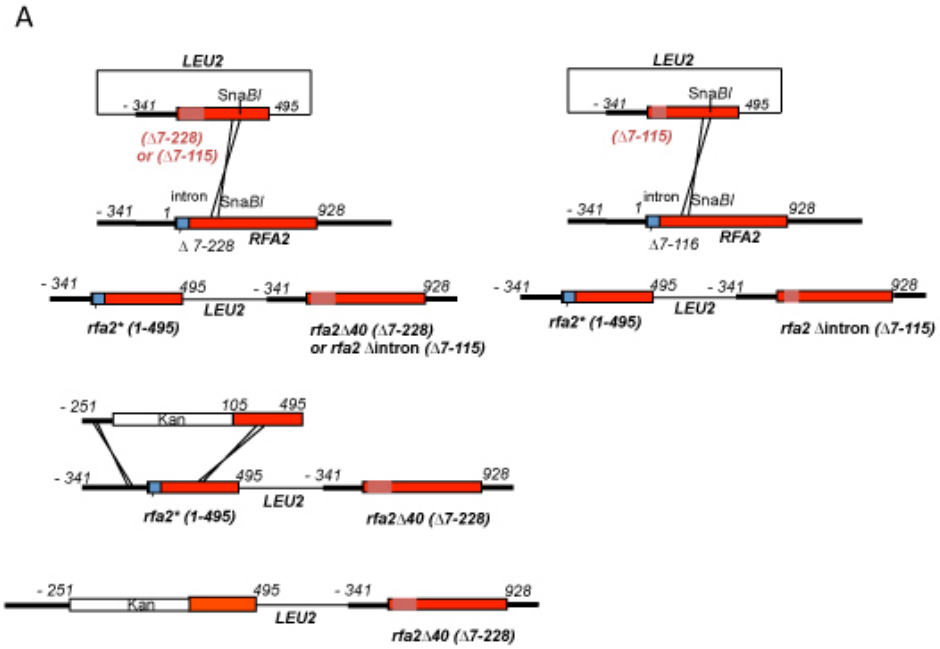

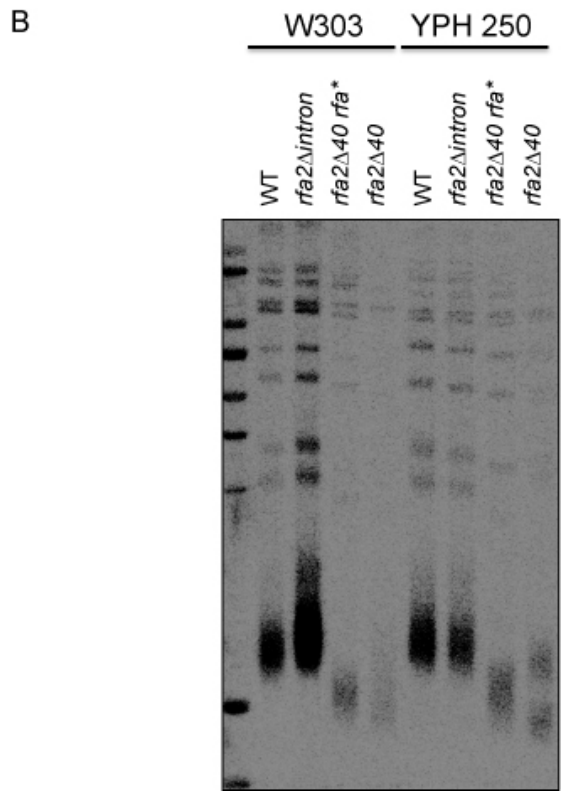

Colonies bearing the *rfa2Δ40* allele are small, crenellated and contain very short telomeres. Many of these cells senesce. Re-streaking *rfa2Δ40* cells produces a high number of cells with wild-type growth and telomere length.

(C) Scheme of the construction of the *rfa2Δ40* allele by a pop-in/pop-out method using FOA selection. *RFA2* with the indicated 5' and 3' regions and containing the deletion *(Δ7-228*) was cloned into the integrative vector pRS306 (A kind gift from K. Friedman). The genomic copy of *RFA2* contains an intron marked with a green box. pRS306-*RFA2(Δ7-228)* was either digested by *Spe*I or *Sna*BI to give the indicated integrations. These integrations create two different duplications containing the wild-type and the mutant copy of *RFA2*. BY4741 (MATa) or BY4742 (MATα) strains containing the two indicated integrations were plated on FOA plates to select for the excision of the *URA3*-plasmid. Successful replacements were checked by PCR, Southern blot and finally by Western blot.

(D) Western blot and Southern blot of BY4741 (MATa) or BY4742 (MATα) strains bearing the *rfa2*Δ*40* allele. Only the clones bearing the *Spe*I pRS306-*RFA2(*Δ*7-228)* integration gave successful replacements. Genomic DNAs of the indicated strains were digested with *Xho*I and hybridized with a TG_{1-3} probe.

C

pS306-*RFA2 (Δ7-228)*

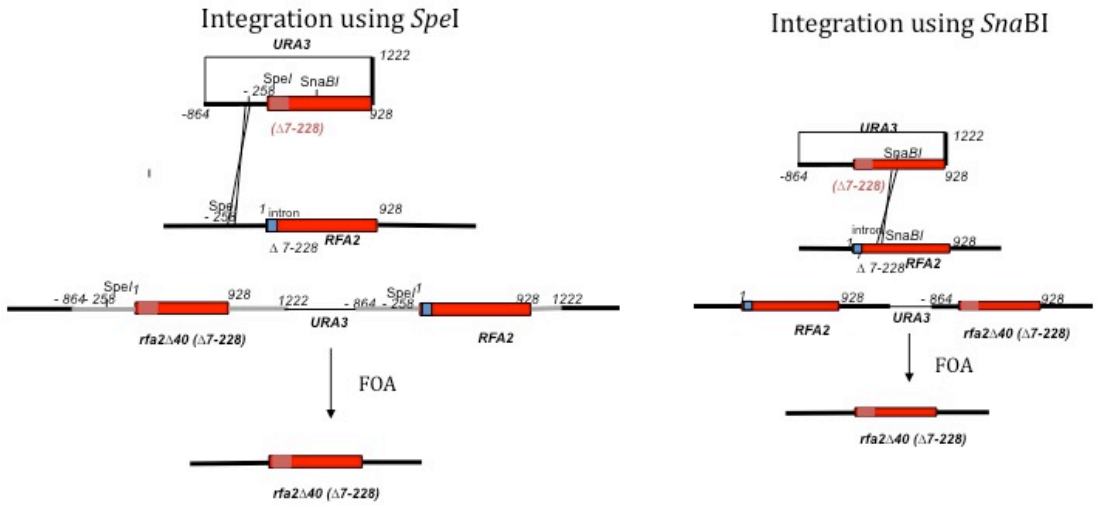

D

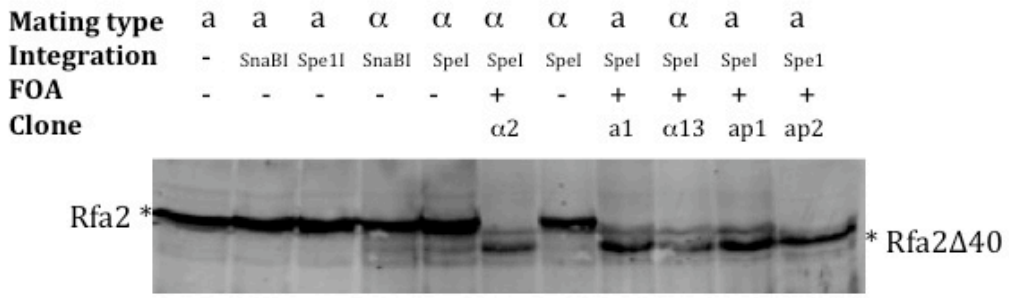

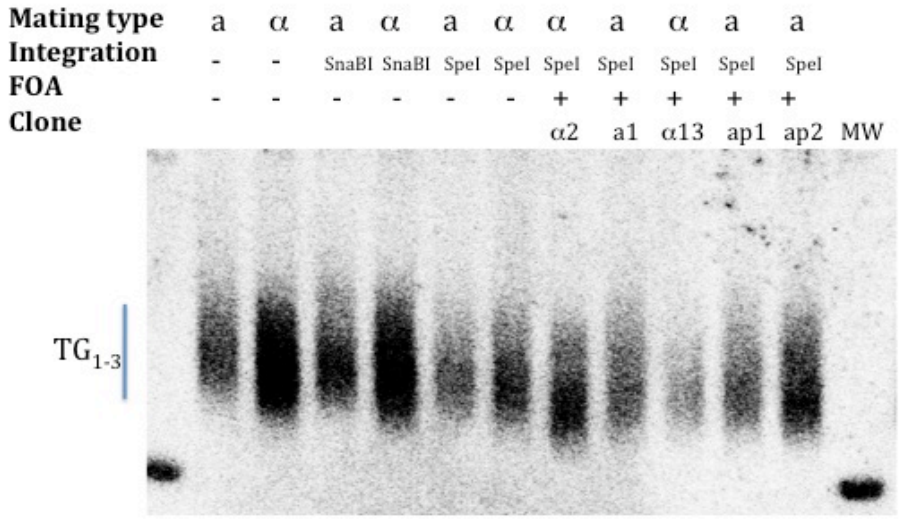

Introducing the *rfa2Δ40* allele by the pop-in/pop-out method using FOA selection leads to a slight reduction of telomere length in contrast of what is observed with the direct integration method (see A and B). This discrepancy is not due to sequence differences. It may be due to a different expression level of the Rfa2Δ40 protein, or alternatively the FOA selection of the pop-in/pop-out method favours the emergence of clones bypassing the *rfa2Δ40* telomere length defect.

Materials and Methods

Yeast strains

A strain W303-1A (*MAT a*, *RFA1-MYC18::TRP1*) was crossed with W303-1B (*MAT alpha, bar1::TRP1 RAD5, URA3-GPD-TK, phENT1-LEU2*). From the dissection of the diploid, *we* isolate a spore PL9T163 with the following

genotype (MAT a, *bar1::TRP1, RFA1-myc18::TRP1, ade2-1, trp1-1, can1-100, leu2-3, 112, his3-11,15, ura3-1, GAL, RAD5+, URA3 GPD-TK, phENT1-LEU2*). This new strain (PL9T163) expresses a functional Rfa1-Myc18, incorporates BrdU and exits from the alpha-factor block more efficiently than the original pp529 strain from Faure et al. 2010. We then disrupted *MRE11* in PL9T163 to give PL9T163 *mre11::HIS3*.

Chromatin Immunoprecipitation (ChIP).

ChIP was performed according to standard procedures. Briefly, 50 ml cultures of yeast cells at an OD_{600} = 1 were fixed with 1% formaldehyde for 15 min, lyzed with glass beads, and the fixed chromatin was fractionated by ultracentrifugation (Beckman Coulter, Villepinte, France). The chromatin fraction was broken by sonication using a Bioruptor (Diagenode, Liège, Belgium). After clearing chromatin by centrifugation at 16000xg for 15 mins, target proteins were immunoprecipitated by specific antibodies overnight and with Dynabeads protein G (Invitrogen Dynal AS, Oslo, Norway) for 3h at 4°C or alternatively with antibody crosslinked to agarose beads. After washing, the chromatin was eluted from the beads at 65°C for 10 min and transferred to a new tube. Cross-links were reversed by incubation at 65°C overnight. DNA was purified using Purelink PCR purification kit (Invitrogen SARL, Cergy Pontoise, France) and eluted in 30 µl of water. Samples were subjected to real-time PCR using a Rotor Gene 6000 (Corbett Research, Labgene, Archamps, France) and Sensimix DNA kit PCR mix (Quantace, Abcys, Paris, France). ChIPs were expressed as a ratio of IP/Input telomeric DNA: IP/Input non telomeric DNA (Gal2A). Immunoprecipitation of cross-linked chromatin was performed with the following antibodies: 9E10 (anti-MYC)-agarose-conjugated monoclonal antibodies (Santa Cruz Biotechnology, Santa Cruz, Ca, USA; anti-FLAG M2 antibody (Sigma, St Quentin Fallavier, France) and anti-RPA2 and anti-RPA1 (S.J. Brill, Rutgers University, NJ, USA).

Cell cycle progression and BrdU labelling

Yeast cultures (1.1 l of SC medium minus leucine) were grown at 30°C to an A_{600} of 0.8 and arrested in G1 with α-factor (100 ng/ml). BrdU (Sigma) was

added to the medium to a final concentration of 100 µg/ml, 30 min before the cells were released from the α-factor block. Cells were washed twice in an equal volume of distilled water and once with fresh SC medium and released into the first cell cycle in 1,1 l of SC medium (minus leucine) at 25°C. After budding of the majority of cell (90%) during the first cell cycle, α-factor (100 ng/ml) was added again to obtain synchronised cells for the second cell cycle. Cells were washed as described above and released in the absence of BrdU into the second cell cycle in SC medium (minus leucine) to obtain an A_{600} of 0.8 at 25°C. Medium is supplemented by Thymidine (Sigma, 500 µg /ml) used as a competitor for the residual internal BrdU (Lengronne et al., 2001). At each time point, samples were collected to check the synchrony of the cell cycle progression by microscopy. At the indicated times, 1ml of cells was fixed in 70% EtOH and two cell samples of 50 ml were collected and fixed with 1% formaldehyde for 15 minutes at RT for FACS and ChIPs analysis, respectively. Cell cycle progression was monitored by flow cytometry using a FACS Calibur (Becton Dickinson).

Detection and quantification of DNA in the ChIP by dot blot assay

DNA (5 µl of input and ChIP DNA) was denaturated in 1.5 N NaOH, 3M NaCl for 10 min at room temperature, spotted directly onto two Hybond-N+ membranes and crosslinked with UV. The membranes were hybridized either with a TG_{1-3} probe or a *GAL2* probe. The signals were quantified with the "Image Gauge" software. The ratios ChIP / Input signal are represented.

Detection and quantification of BrdU by dot blot assay

DNA (2 µl of input and 20 µl of ChIP DNA) was denaturated in 1.5 N NaOH, 3M NaCl for 10 min at room temperature and spotted directly onto a nitrocellulose membrane (Protran). The membrane was crosslinked with UV and blocked for 30 min at room temperature in TBS 1X, 0.1% Tween-20, 5% milk. The membrane was then incubated with a monoclonal antibody against BrdU (1:3000; Abcam ab12219) for 1 hour at room temperature in TBS1X, 0.1% Tween-20, 0.1% milk. An Alexa Fluor 780 anti-mouse goat IgG (1:5000;

Molecular Probes) was used as a secondary antibody. Fluorescence was detected and quantified using an Odyssey Imager (LI-COR Bioscience). BrdU incorporation was plotted as the signal of each dot normalized to the higher BrdU signal. The BrdU immunoprecipitated with the ChIP at each time point is normalized to the corresponding input signal.

Table S1
Oligonucleotides:

GAL2A	5'-GTTAAGCCCTTCCCATCTCAA-3' 5'-ATCTCCACATTTTAGCCTGCG-3'
ARO1	5'-CAGCAATTAGTCCTGGAATTCAAGG-3' 5'-GTCAATTGATTGGTAACCTTGACAT-3'
Chromo VI- L	5'-ACGTTTAGCTGAGTTTAACGGTG-3' 5'-CATGACCAGTCCTCATTTCCATC-3'
Chromo XV-L	5'-TAACCCTGTCCAACCTGTCT-3' 5'-ATACTATAGCATCCGTGGGC-3'
TLC1	T3 : 5'-CATAAAGTGACAGCGCTTAG-3' T5 : 5'-CTCGATGGTGAAGAGATAGT-3'
TER1	5'-Ter1 : 5'GTGCAGTGTACGTGAGTCTTCTGCCT-3' 3'-Ter1 : 5'-GATCCATGGATCTCACGTAATG-3'
Telo pombe Moser *et al*., 2009	5'-Telo: 5'-TATTTCTTTATTCAACTTACCGCACTTC-3' 3'-Telo: 5'-CAGTAGTGCAGTGTATTATGATAATTAAAATGG-3'
NonTelo pombe Moser *et al*., 2009	5'-nonARS-70F: 5'-TACGCGACGAACCTTGCATAT-3' 3'- nonARS-70R: 5'-TTATCAGACCATGGAGCCCATT-3'

Table S2

S. cerevisiae strains:

S. cerevisiae strains	Genotype	Origin
W303-1A	*MAT* ***a*** *ade2-1 can1-100 his3-11, 15 leu2-3-112 trp1-1 ura3*	M.P. Longhese
W303 EST2-myc18	*MAT* ***a*** *ade2-1 can1-100 his3-11, 15 leu2-3-112 trp1-1 ura3 EST2-18-myc ::*HIS3	V. Géli
W303 EST1-myc13	*MAT* ***a*** *ade2-1 can1-100 his3-11, 15 leu2-3-112 trp1-1 ura3 EST1-13-myc ::*TRP1	This study
W303 *CDC13-myc18*	*MAT* ***a*** *ade2-1 can1-100 his3-11, 15 leu2-3-112 trp1-1 ura3 CDC13-18-myc :: TRP1*	This study
W03 *yKU80-myc13*	*MAT* ***a*** *ade2-1 can1-100 his3-11, 15 leu2-3-112 trp1-1 yKUu80-13-myc :: TRP1 bar1 :: URA3*	This study
YAB 885	*MAT* ***a*** *ade2-1 his3-11,15 leu2-3,115 trp1-1 ura3-1 can1-100 RAD5 RIF1-13-myc :: HIS3*	A. Bianchi
W303 *RIF1-myc13*	*MAT* ***a*** *ade2-1 can1-100 his3-11, 15 leu2-3-112 trp1-1 ura3 RIF1-13-myc :: HIS3 (from cross YAB885*W303)*	This study
W303 *RFA1*-myc18 (K7120)	*MAT* ***a*** *ade2-1 can1-100 his3-11, 15 leu2-3-112 trp1-1 ura3 RFA1-18-myc ::*TRP1	K. Nasmyth
W303 *mre11*Δ	MAT **a** *ade2-1 can1-100 his3-11, 15 leu2-3-112 trp1-1 mre11::* TRP1 *bar1 ::URA3*	This study
W303 *rfa1D228Y (*W1479-18C)	*MAT::HIS3* lys2ΔSpeI RAD5 leu2 EcoRI::URA3HOcs::leu2ΔBstEII *rfa1-D228Y*	(Smith and Rothstein, 1999)
W303 *CDC13-flag*	*MAT* ***a*** *ade2-1 can1-100 his3-11, 15 leu2-3-112 trp1-1 CDC13-Flag :: KAN bar1 ::URA3*	This study
W303 *CDC13-flag mre11*Δ	*MAT* ***a*** *ade2-1 can1-100 his3-11, 15 leu2-3-112 trp1-1 CDC13-Flag :: KAN mre11::* TRP1 *bar1 ::URA3*	This study
W303 *rfa1D228Y*	*MAT* ***a*** *ade2-1 can1-100 his3-11, 15 leu2-3-112 trp1-1 rfa1D228Y bar1 ::URA3*	This study
W303 *rfa1D228Y CDC13-Flag*	*MAT* ***a*** *ade2-1 can1-100 his3-11, 15 leu2-3-112 trp1-1 CDC13-Flag :: KAN rfa1-D228Y bar1 ::URA3*	This study
W303 *rfa1-D228Y yKU80-13-myc*	*MAT* ***a*** *ade2-1 can1-100 his3-11, 15 leu2-3-112 trp1-1 yKU80-13-myc :: TRP1* rfa1-D228Y	
PP529b	*MAT* ***a****, ade2-1, trp1-1, can1-100, leu2-3, 112, his3-11,15, ura3-1, GAL, psi+, RAD5, URA3 GPD-TK, phENT1-LEU2 bar1::TRP1*	P. Pasero
PL9T163	MAT **a**, *bar1::TRP1, RFA1-myc18::TRP1, ade2-1, trp1-1, can1-100, leu2-3, 112, his3-11,15, ura3-1, GAL, RAD5+, URA3 GPD-TK, phENT1-LEU2*	This study

PL9T163 *mre11Δ*	MAT **a**, *bar1::TRP1, RFA1-myc18::TRP1, mre11::HIS3 ade2-1, trp1-1, can1-100, leu2-3, 112, his3-11,15, ura3-1, GAL, RAD5+, URA3 GPD-TK, phENT1-LEU2*	This study
YTSF73	Mat ***a/α*** *TEL::URA3/VII-L tlc1Δ48/ TLC1* cdc13-2*/CDC13 EST1-Myc9::TRP1/EST1*	V. Zakian
YTSF74	Mat ***a/α*** *TEL::URA3/VII-L tlc1Δ48/TLC1 est1::HIS3-EST1*	V. Zakian
YPH499 *cdc13-2*	Mat ***a*** *TEL::URA3/VII-L cdc13-2*	V. Zakian
YPH499 *est1Δ*	Mat ***a*** *TEL::URA3/VII-L est1::HIS3*	V. Zakian
YPH499 *tlc1Δ48*	Mat ***a*** *TEL::URA3/VII-L tlc1Δ48*	V. Zakian
YPH499 *cdc13-2 tlc1Δ48*	Mat ***a*** *TEL::URA3/VII-L cdc13-2 tlc1Δ48*	V. Zakian
YPH499 *est1Δ tlc1Δ48*	Mat ***a*** *TEL::URA3/VII-L est1::HIS3 tlc1Δ48*	V. Zakian
Ybp110 W303 *rif1Δ rif2Δ*	Mat ***a*** *bar1 rif1::NAT rif2::HPH*	Marcand
W303 *rif1Δ rif2Δ rfa1-D228Y*	Mat ***a*** *bar1 rif1::NAT rif2::HPH rfa1-D228Y*	This study
W303 *rif1Δ*	Mat ***a*** *bar1 rif1::NAT*	S. Marcand
W303 *rif1Δ rfa1Δ228Y*	Mat ***a*** *bar1 rif1::NAT rfa1-D228Y*	This study
W303 *rif2Δ*	Mat ***a*** *bar1 rif2::HPH*	S. Marcand
W303 *rif2Δ rfa1-D228Y*	Mat ***a*** *bar1 rif2::HPH rfa1-D228Y*	This study
W303 CDC13-MYC13	MAT **a** *ade2-1 can1-100 his3-11, 15 leu2-3-112 trp1-1 ura3* CDC13-MYC13::HIS3	This study
W303 *rif1Δ rif2Δ*	MAT **a** *bar1 ade2-1 can1-100 his3-11, 15 leu2-3-112 trp1-1 ura3 rif1::NAT rif2::HPH*	S. Marcand
W303 CDC13-MYC13 *rif1Δ rif2Δ*	MAT **a** *ade2-1 can1-100 his3-11, 15 leu2-3-112 trp1-1 ura3* CDC13-MYC13::HIS3 *rif1::NAT rif2::HPH*	This study

S. pombe strains:

S. pombe strains	Genotype	Origin
972h wild-type	*h- leu1-32 ura4-D18*	P. Russell
SC36	*h- leu1-32 ura4-D18 slx1-13myc::kanMX6*	S. Coulon
YO 004 (SC233)	*h+ leu1-32 ura4-D18 ade6-M210 rad11-13myc::kanMX6*	M. Ueno
YO 008 (SC234)	*h+ leu1-32 ura4-D18 ade6-M210 rad11-D223Y-13myc::kanMX6*	M. Ueno
SC246	*leu1-32 ura4-D18 ade6-M210 cdc25-22 rad11-D223Y-13myc::kanMX6*	This study
JCF1301	*h- leu1-32 ura4-D18 ade6-M210 his3-D1 cdc25-22*	J. Cooper
YO009 (SC235)	*h+ leu1-32 ura4-D18 ade6-M210 cdc25-22 rad11-13myc::kanMX6*	M. Ueno

JCF1341 (SC238)	*h+ leu1-32 ura4-D18 ade6-M210 est1-V5::kanMX6*	J. Cooper
JCF1302 (SC239)	*h+ leu1-32 ura4-D18 ade6-M210 cdc25-22 est1-V5::kanMX6*	J. Cooper
SC345	*leu1-32 ura4-D18 tel1::leu2 rad11-13myc::kanMX6*	This study
SC347	*leu1-32 ura4-D18 rad3::leu2 rad11-13myc::kanMX6*	This study
TN1678 (SC414)	*h- leu1-32 ura4-D18 ade6-M210 rad3::kanMx4* (Kinase delete)	T. Nakamura
TN1374 (SC334)	*h- leu1-32 ura4-D18 ade6-M210 rad3::leu2*	T. Nakamura
SC433, 434, 435	*leu1-32 ura4-D18 ade6-M210 rad3::leu2 rad11-D223Y*	This study
YTC6879 (SC396)	*h- leu1-32 ura4-D18 ade6-M210 poz1::kanMx6*	T. Nakamura
SC490, 491	*leu1-32 ura4-D18 poz1::kanMx6 rad11-D223Y*	This study
JK774 (SC392)	*h- leu1-32 ura4-D18 rap1::ura4*	F. Ishikawa
SC486, 4876, 488	*h- leu1-32 ura4-D18 rap1::ura4 rad11-D223Y*	This study
SC501, 502	*h- leu1-32 ura4-D18 poz1::kanMx6 rad3::kanMx4* (Kinase delete)	This study

Supplemental References :

Faure V., Coulon S., Hardy J. and Géli V. 2010. The telomeric single-stranded DNA-binding protein Cdc13 and telomerase bind through different mechanisms at the lagging- and leading-strand telomeres. *Molecular Cell* **38**: 842-853.

Bochkareva E., Belegu V., Korolev S. and Bochkarev A. 2001. Structure of the major single-stranded DNA-binding domain of replication protein A suggests a dynamic mechanism for DNA binding. EMBO J. 20:612-8.

Bochkareva E., Korolev S., Lees-Miller S.P. and Bochkarev A. 2002. Structure of the RPA trimerization core and its role in the multistep DNA-binding mechanism of RPA. *EMBO J*. **21**:1855-63.

Schramke, V., Luciano, P., Brevet, V., Guillot, S., Corda, Y., Longhese, M.P., Gilson, E., and Geli, V. 2004. RPA regulates telomerase action by providing Est1p access to chromosome ends. *Nat Genet* 36: 46-54.

Lengronne A**.**, Pasero P**.**, Bensimon A**.** and Schwob E. 2001. Monitoring S phase progression globally and locally using BrdU incorporation in TK(+) yeast strains. Nucleic Acids Res. 29:1433-42.

Moser, B.A., Subramanian, L., Chang, Y.T., Noguchi, C., Noguchi, E., and Nakamura, T.M. 2009. Differential arrival of leading and lagging strand DNA polymerases at fission yeast telomeres. *EMBO journal* 28: 810-820.

Smith J, Rothstein R. An allele of RFA1 suppresses RAD52-dependent double-strand break repair in Saccharomyces cerevisiae.Genetics. 1999 Feb;151(2):447-58.